

Chirality dependence of the thermal conductivity of carbon nanotubes

This article has been downloaded from IOPscience. Please scroll down to see the full text article.

2004 Nanotechnology 15 936

(<http://iopscience.iop.org/0957-4484/15/8/010>)

View [the table of contents for this issue](#), or go to the [journal homepage](#) for more

Download details:

IP Address: 210.72.8.28

The article was downloaded on 31/03/2012 at 06:07

Please note that [terms and conditions apply](#).

Chirality dependence of the thermal conductivity of carbon nanotubes

Wei Zhang¹, Zhiyuan Zhu¹, Feng Wang², Tingtai Wang¹,
Litao Sun¹ and Zhenxia Wang¹

¹ Shanghai Institute of Applied Physics, Chinese Academy of Sciences, Shanghai 201800, People's Republic of China

² Department of Physics, Beijing Institute of Technology, Beijing 100081, People's Republic of China

E-mail: zhangw@sinr.ac.cn

Received 17 January 2004

Published 9 June 2004

Online at stacks.iop.org/Nano/15/936

doi:10.1088/0957-4484/15/8/010

Abstract

The thermal conductivities of three types of single-wall carbon nanotubes are studied using the homogeneous non-equilibrium Green–Kubo method based on the Brenner potential. The thermal conductivity of a carbon nanotube is found to have dependence on its chirality. The thermal conductivities of three types of nanotube seem to have similar temperature dependence. The thermal conductivity of the chiral nanotube is lower than that of the other two types of nanotube.

With the rapid progress of the synthesis and processing of nanoscale structure material, there has emerged a demand to study the thermal transport process in nanoscale structures, nanoscale devices and nanostructured materials. Since the discovery of carbon nanotubes (CNTs) by Iijima *et al* [1], their mechanical and electronic properties have been well studied. However, the thermal conductivity of CNTs has not been fully understood until now. Because of their decreasing size, nanoscale systems present difficulties for direct measurement. Several experiments [2, 3] have studied the thermal conductivities of CNTs. But because of the strong dependence of thermal conductivity on the thermal phonon mean free path, the experiments have an unusual sensitivity to isotopic and other atomic defects. So far, no analytical theories have adequately treated the thermal transport problem in the nanoscale. Computational approaches span the range from numerical solutions of Fourier's law to calculations based on the Boltzmann transport equation to atomic level simulations [4]. Compared with other methods, the MD approach does not require any *a priori* understanding of heat transports, so it is ideal for investigating the fundamental heat-transfer mechanisms themselves.

Several works [5–7] have studied the thermal transport properties of single-wall CNTs using molecular dynamics. There have been three methods for calculating the thermal conductivity of CNT: the equilibrium Green–Kubo (EGK)

method [5], the direct method [6] and the homogenous non-equilibrium Green–Kubo (HNEGK) method [7]. The EGK and direct methods give similar results. However the HNEGK method based on the Tersoff potential [8] gives an unusually high value. Now, zigzag and armchair type nanotubes have been studied, but there have been no calculations of chiral CNTs. Compared with graphite and diamond, carbon nanotubes have a high thermal conductivity. The thermal conductivity of CNTs is dependent on the temperature and their diameter.

The direct method mimics the natural thermal transport process, and calculates the thermal conductivity through Fourier's law. For the direct method the use of large temperature gradients required ($\sim 10^9$ K m⁻¹) could introduce significant nonlinear effects, and the definition of temperature in the small parts of the nanoscale system when calculating the gradients of temperature is quite a problem. But it is convenient to study thermal conductance of interfaces. The idea of the EGK method is that the linear response coefficients can be calculated through the fluctuations of the flux related to the conductivity in equilibrium states. For the EGK method, by contrast with the direct method, one is always assured of being in the linear-response regime. But the computational demand is quite large due to the slow convergence of the autocorrelation function, requiring long integration time periods. Both methods have finite-size effects [9]. Nevertheless, when finite-size effects are treated correctly and sufficiently long

simulations are performed, the EGK method and the direct method are indeed consistent with each other [9].

The idea of the HNEGK method is that a non-equilibrium system can be modelled as a perturbed equilibrium ensemble. The perturbing field does work on the system and prevents the system from relaxing to equilibrium. The work is converted to heat, and the heat must be removed in order to obtain a well defined steady state. Studying the steady non-equilibrium state, one can get the nonlinear response coefficients. The linear response coefficients can be obtained by extrapolating the results to zero field. The HNEGK method does not have as big computational requirements as the EGK method; it is efficient for calculation of the thermal conductivity of nanoscale samples.

In our simulation we use the HNEGK method based on the Brenner potential [10]. Our results indicate that the HNEGK method gives similar results to other methods, and the thermal conductivity of a nanotube not only depends on its length and radius, but also depends on its chirality. Our results suggest that a nanoscale device with different heat conductivity may be made with nanotubes of different chirality.

For CNTs, the electronic contribution to the thermal conductivity is expected to be negligible due to the low density of free charge carriers [11, 12]. For example, Benedict *et al* [13] showed that the phonon contribution was dominant down to 0 K and that the phonon contribution to the heat capacity was 10 000 times larger than the electronic contribution. So in our work, only the phonon contribution is considered.

The macroscopic thermal conductivity of a solid along a particular direction, taken here as the z axis, is defined through Fourier's law of heat conduction as

$$\frac{1}{A} \frac{dQ}{dt} = -\lambda \frac{dT}{dz}, \quad (1)$$

where dQ is the quantity of heat transmitted across the area A in the time interval dt .

In an equilibrium system, Green–Kubo formula takes the form

$$\lambda = \frac{1}{3Vk_B T^2} \int_0^\infty \langle J(t) \cdot J(0) \rangle dt \quad (2)$$

where k_B is the Boltzmann constant, V is the volume, T is the temperature of the sample and the angular brackets denote an ensemble average. The microscopic heat flux vector $J(t)$ is defined by

$$J(t) = \frac{d}{dt} \sum_i r_i \nabla e_i = \sum_i v_i \Delta e_i - \frac{1}{2} \sum_i \sum_j r_{ij} (f_{ij} \cdot v_i) \quad (3)$$

where $\Delta e_i = e_i - \langle e \rangle$ is the excess energy of atom i with respect to the average energy per atom $\langle e \rangle$. r_i , v_i are the position and velocity of atom i , respectively, and $r_{ij} = r_j - r_i$. Assuming that the total potential energy $U = \sum_i u_i$ can be expressed as a sum of binding energies u_i of individual atoms, then $f_{ij} = -\nabla_i u_j$, where ∇_i is the gradient with respect to the position of atom i .

According to the linear response theory [14], for a small fictitious thermal force (with a dimension of inverse length), $|F(s)| \rightarrow 0$, there exists the expression

$$\langle J(t) \rangle = -\beta V^2 \int_0^t ds \langle J(t-s)J \rangle \cdot F(s). \quad (4)$$

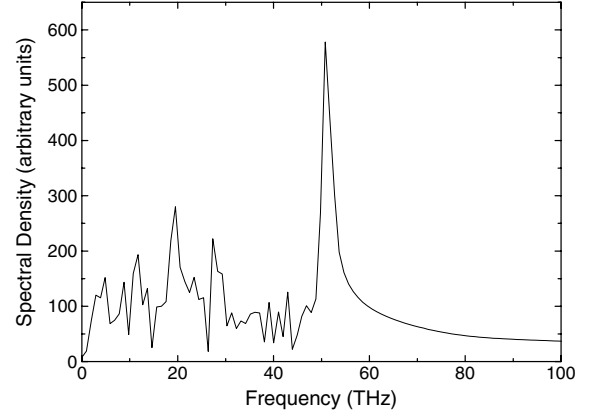


Figure 1. Phonon spectrum of the (10, 10) nanotube calculated from the Fourier transform of the velocity auto-correlation function generated during the simulations.

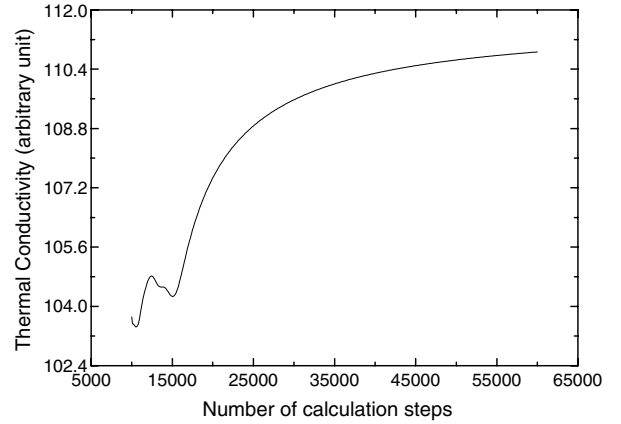


Figure 2. The converging behaviour of the thermal conductivity of a (11, 11) nanotube with increasing number calculation steps, for $F_e = 0.3 \text{ \AA}^{-1}$, at temperature $T = 300 \text{ K}$.

Here $\beta = 3N/2k_B$, and N is the number of atoms in the studied system. So, the Green–Kubo formula becomes

$$\lambda = \lim_{F_e \rightarrow 0} \lim_{t \rightarrow \infty} \frac{\langle J_z(F_e, t) \rangle}{F_e T V} \quad (5)$$

where T is the temperature of the sample, regulated by a Nosé–Hoover thermostat [15]. The equations of motion are

$$\begin{aligned} \dot{r}_i &= p_i/m \\ \dot{p}_i &= \sum_j f_{ij} + \Delta e_i F_e - \frac{1}{2} \sum_j F_{ij} [r_{ij} \cdot F_e] \\ &\quad + \frac{1}{2N} \sum_{j,k} f_{jk} [r_{jk} \cdot F_e] - \alpha p_i. \end{aligned} \quad (6)$$

Here, α is the Nosé–Hoover thermostat multiplier acting on the momentum p_i of atom i .

In our simulation, the Brenner potential is augmented by the Lennard-Jones potential, which simulates the van der Waals interactions between carbon atoms. The Brenner potential is widely used in modelling carbon based systems, such as diamond, graphite, fullerenes and CNTs. The suitability of the Brenner potential for these simulations is checked by comparing the phonon spectrum computed during the

simulation with the experiment in plane graphite phonon modes. In figure 1, the phonon spectrum shows a strong peak around 50 THz which is characteristic of the graphite phonon spectrum.

In our simulation, (10, 10), (11, 11), (20, 0), (10, 13) nanotubes are studied. The last three tubes have nearly equal radii, which is convenient for comparison. The cross-sectional area of the single-wall nanotube is taken to be an annular ring of thickness 3.4 Å. Periodic conditions are used to model infinite long systems. There are 528, 480, 532 atoms, respectively in the simulation boxes for (11, 11), (20, 0), (10, 13) nanotubes. The time step is 0.5 fs in our simulation. Each simulation run consists of 60 000 steps, which is enough to make the heat flux converge. The converging behaviour can be seen in figure 2.

In order to compare our result with the results of other methods [5–7], we calculated the temperature dependence of (10, 10) CNTs. The result is shown in figure 3. From figure 3 it can be seen that in our result the temperature dependence of thermal conductivity of a (10, 10) nanotube is similar to the result of [6]. However, the peak emerges at a higher value.

In figure 4 we give the temperature dependences of the thermal conductivities of three types of nanotube. The behaviour of conductivity of a (11, 11) nanotube with respect to temperature is similar to that of a (10, 10) nanotube, however the (10, 10) nanotube has a peak at 500 K while the (11, 11) nanotube has a peak at 400 K. The value of the thermal conductivity of the (11, 11) nanotube is much higher than that of the (10, 10) nanotube.

It can be seen from figure 4 that the temperature dependences of all types of CNTs show similar behaviour with increasing temperature. They all have a peak in the range from 100 to 500 K. In the range from 100 to 400 K, the conductivity of the (11, 11) nanotube is lower than that of the (20, 0) nanotube. But compared with other types of nanotubes, the (10, 13) nanotube has a lower value of thermal conductivity. Provided the numbers of the three types of nanotube are equal in a single-wall nanotube bulk sample, the thermal conductivity of the bulk increases with the temperature increase in the range from 0 to 300 K. This is in agreement with the result in [2].

Thermal resistance is caused by phonon–phonon interaction known as Umklapp process (U-process). U-processes refer to phonon–phonon scattering processes where the final state wavevectors lie outside the Brillouin zone. Whether the final phonon exceeds the Brillouin zone depends on the magnitude of the three components of the wavevector. The axial component remains independent of tube diameter, and all tubes has the same distribution of axial component. But in smaller diameter nanotubes, the radial and azimuthal components are larger than those in larger diameter nanotubes. Thus the U-process takes place more easily in small diameter nanotubes. This is the reason why the thermal conductivity of the (10, 10) nanotube is lower than the (11, 11) nanotube [6].

In armchair and chiral (10, 13) nanotubes the sigma bonds along the circumference are strongly strained, while in zigzag nanotubes they are not. The sigma bond along the zigzag tube axis has the least strain. It is known that in solids where the phonon contribution to the thermal conduct dominates, the thermal conductivity is proportional to Cvl , in which C is the heat capacity per volume, v is the speed of sound, l is the mean free path. The excess strain along the circumference in

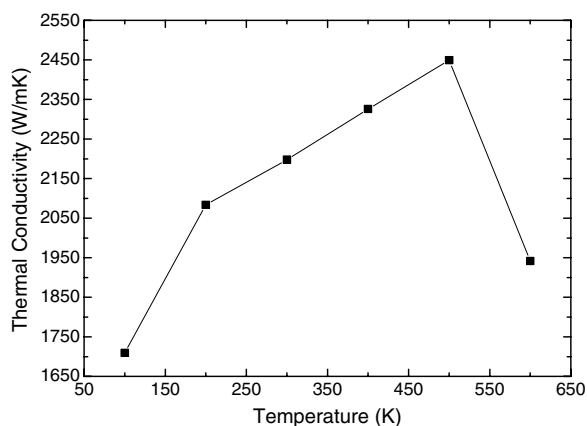


Figure 3. Thermal conductivities of a (10, 10) nanotube.

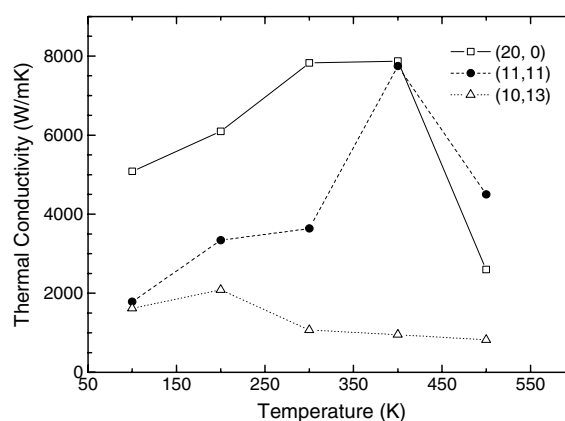


Figure 4. Thermal conductivities of (20, 0)—open squares, (11, 11)—solid circles, and (10, 13)—open triangles, nanotubes.

armchair and chiral nanotubes can limit the phonon mean free path due to scattering and lower the thermal conductivity. Thus the conductivities of armchair and chiral nanotubes are lower than that of the zigzag nanotube.

In armchair and zigzag nanotubes, the atom chains are parallel to the axis, but in chiral nanotubes, the atom chains are not parallel to the axis, instead they are in a helix. Thus the vibration of the atoms chain in chiral nanotubes is apt to have a long path, and may easily transfer the momentum to the radial direction, which causes the low thermal conductivity of chiral nanotubes.

In summary, we have calculated the thermal conductivities of three types of CNTs, using the homogeneous non-equilibrium Green–Kubo method based on the Brenner potential. We find that the thermal conductivity of single wall CNTs is not only related to their radii and the temperature, but also related to their chirality. The zigzag nanotube has a maximum value and the chiral nanotube has a minimum value. The three types of nanotubes show similar temperature dependence.

Acknowledgment

This work is partially supported by the Key Project of the Knowledge Innovation Programme of the Chinese Academy of Sciences.

References

- [1] Iijima S 1991 *Nature* **354** 56
- [2] Hone J, Whitney M, Piskori C and Zettl A 1999 *Phys. Rev. B* **59** R2514
- [3] Kim P, Shi L, Majumdar A and McEuen P L 2001 *Phys. Rev. Lett.* **87** 215502
- [4] Cahill D G, Ford W K, Goodson K E, Mahan G D, Majumdar A, Maris H J, Merlin R and Phillpot S R 2003 *J. Appl. Phys.* **93** 793
- [5] Che J, Cagin T and Goddard W A III 2000 *Nanotechnology* **11** 65
- [6] Osman M A and Srivastava D 2001 *Nanotechnology* **12** 21
- [7] Berber S, Kwon Y-K and Tomanek D 2000 *Phys. Rev. Lett.* **84** 4613
- [8] Tersoff J 1988 *Phys. Rev. B* **37** 6991
- [9] Schelling P K, Phillpot S R and Keblinski P 2002 *Phys. Rev. B* **65** 144306
- [10] Brenner D W 1990 *Phys. Rev. B* **42** 9458
- [11] Hone J, Llaguno M C, Nemes N M, Johnson A T, Fisher J E, Walters D A, Casavant M J, Schmidt J and Smalley R E 2000 *Appl. Phys. Lett.* **77** 666
- [12] Kelly B T 1981 *Physics of Graphite* (Englewood Cliffs, NJ: Applied Science) p 249
- [13] Benedict L X, Louie S T and Cohn M L 1996 *Solid State Commun.* 100 and 177
- [14] Hansen D P and Evans D J 1994 *Mol. Phys.* **81** 767
- [15] Nosé S 1984 *Mol. Phys.* **52** 255
- Hoover W G 1985 *Phys. Rev. A* **31** 1695